Author(s): Jääskeläinen, Sirpa; Koskinen, Laura; Kultamaa, Matti; Haukka, Matti; Hirva, Pipsa

Title: Persistence of oxidation state III of gold in thione coordination

Year: 2017

Version:

Please cite the original version:

Jääskeläinen, S., Koskinen, L., Kultamaa, M., Haukka, M., & Hirva, P. (2017). Persistence of oxidation state III of gold in thione coordination. Solid State Sciences, 67, 37-45. https://doi.org/10.1016/j.solidstatesciences.2017.03.008

Accepted Manuscript

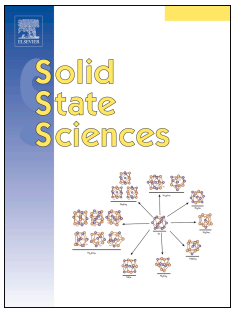

Persistence of oxidation state III of gold in thione coordination

Sirpa Jääskeläinen, Laura Koskinen, Matti Kultamaa, Matti Haukka, Pipsa Hirva

PII: S1293-2558(16)30567-2

DOI: 10.1016/j.solidstatesciences.2017.03.008

Reference: SSSCIE 5476

To appear in: *Solid State Sciences*

Received Date: 16 August 2016

Revised Date: 10 January 2017

Accepted Date: 11 March 2017

Please cite this article as: S. Jääskeläinen, L. Koskinen, M. Kultamaa, M. Haukka, P. Hirva, Persistence of oxidation state III of gold in thione coordination, *Solid State Sciences* (2017), doi: 10.1016/j.solidstatesciences.2017.03.008.

Persistence of oxidation state III of gold in thione coordination.

Sirpa Jääskeläinen[a,*], Laura Koskinen[a], Matti Kultamaa[a], Matti Haukka[b] and Pipsa Hirva[a]

[a] Department of Chemistry, University of Eastern Finland, Joensuu Campus, P.O. Box 111, FI-80101 Joensuu, Finland

[b] Department of Chemistry, University of Jyväskylä, P.O. Box 35, FI-40014 Jyväskylä, Finland

[*]Corresponding author. Tel. +358 505689428. E-mail address: sirpa.jaaskelainen@uef.fi

Graphical abstract

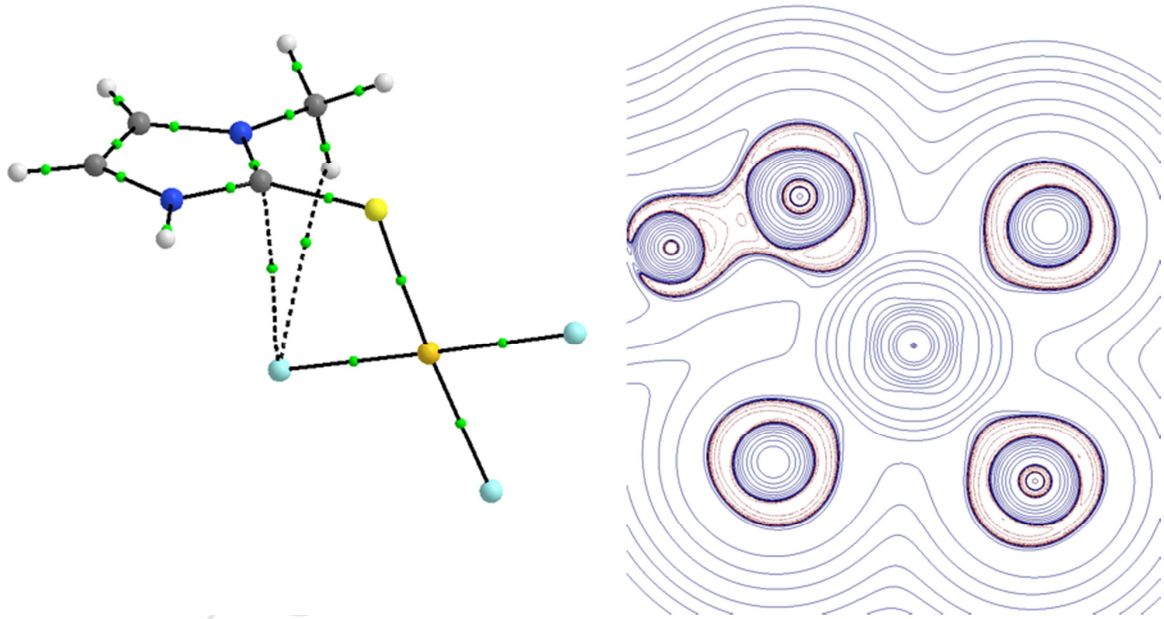

Persistence of oxidation state III of gold in thione coordination.

Sirpa Jääskeläinen[a,*], Laura Koskinen[a], Matti Kultamaa[a], Matti Haukka[b] and Pipsa Hirva[a]

[a] Department of Chemistry, University of Eastern Finland, Joensuu Campus, P.O. Box 111, FI-80101 Joensuu, Finland

[b] Department of Chemistry, University of Jyväskylä, P.O. Box 35, FI-40014 Jyväskylä, Finland

[*]Corresponding author. Tel. +358 505689428. E-mail address: sirpa.jaaskelainen@uef.fi

Abstract

Ligands N,N´-tetramethylthiourea and 2-mercapto-1-methyl-imidazole form stable Au(III) complexes [$AuCl_3$(N,N´-tetramethylthiourea)] (1) and [$AuCl_3$(2-mercapto-1-methyl-imidazole)] (2) instead of reducing the Au(III) metal center into Au(I), which would be typical for the attachment of sulfur donors. Compounds **1** and **2** were characterized by spectroscopic methods and by X-ray crystallography. The spectroscopic details were explained by simulation of the UV-Vis spectra via the TD-DFT method. Additionally, computational DFT studies were performed in order to find the reason for the unusual oxidation state in the crystalline materials. The preference for Au(III) can be explained *via* various weak intra- and intermolecular interactions present in the solid state structures. The nature of the interactions was further investigated by topological charge density analysis via the QTAIM method.

- Thione derivatives of gold were synthesized and characterized
- Oxidation state III was atypically maintained
- Computational TD-DFT studies were used to explain spectroscopic data
- DFT and QTAIM methods were employed to clarify the oxidation state of the metal and the weak interactions in solid state

Keywords: Gold(III), tetramethylthiourea, thione, DFT, QTAIM

1. Introduction

The chemistry of gold at oxidation state I is an area of intense practical and theoretical studies, especially in medicinal and photochemical applications. However, the chemistry of gold(III) complexes is less studied than that of gold(I), mainly due to their notorious toxicity and lower solubility and stability in aqueous media. Although gold at oxidation state I has been used in most studies of biochemical and pharmaceutical applications, Au(III), isostructural with Pt(II), has lately begun to receive more attention. For example, the combination of Au^{3+} with antibiotics has offered promising results against resistant bacteria and seems to serve a broad range of medical applications.[1] High cytotoxicity of some Au(III) derivatives towards cancer cells at low concentrations has also been discovered.[2,3,4,5]

Reduction of gold(III) to gold(I) species is often involved in reactions with soft nucleophiles, such as sulfur compounds. The reduction mechanism and kinetics have been studied in greater detail, e.g. for thioethers and thiocyanate. Coordination has been found to proceed *via* a direct two-electron transfer without observable intermediates. Another possibility includes at the first stage a substitution of, for example, the halogen by the ligand. Further attack of the ligand leads finally to the reduction of the metal center.[6,7,8] Consequently, reactions of both Au(I) and Au(III) species with monodentate heterocyclic thiones[9] and thiourea derivatives[10] typically give linear gold(I) complexes [AuXL] (X=Cl, Br) or $[AuL_2]^+$. For example, the reductive halide substitution by basic thiourea of the metal in $[AuBr_4]^-$ or $[AuCl_4]^-$ has led to formation of $[Au(thiourea)_2]^+$ with counter-ions Br^- [11], Cl^- , SO_4^{2-} [12] or ClO_4^- [13]. The solid state structures were found to constitute linear S-Au-S moieties, which is typical for Au(I) compounds. Moreover, in the solid state structure of $[Au(thiourea)_2]^+Br^-$ the Au atoms formed a linear chain-like arrangement with Au···Au interactions of adjacent units.

However, variation in the reaction type has been observed. Fabretti et al. have studied the reaction between tetramethylthiourea and gold(III), where the expected process of ligand attachment and consecutive reduction gave [Au(I)Br(tetramethylthiourea)]. Distinct behavior and additional formation of $[Au(tetramethylthiourea)_2Br_2][AuBr_2]$ was found. The structure consists of ionic units, where the gold atoms are four and two coordinated. The tetramethylthiourea ligands are *trans* coordinated to the gold(III) in the cationic part together with two bromide ligands forming square planar geometry. The anionic part is linearly coordinated dibromoaurate(I).[14] Tetramethylthiourea seems to be a ligand offering competitive reaction routes and variation of products.

Among the gold(III) compounds with sulfur ligands, some solid state structures of thioether derivatives of Au(III)X_3-SR_2[15,16,17,18,19] have been reported, but the studies have mostly concentrated on solution chemistry and characterization with spectroscopic methods.[20] A large number of mixed ligand species of the type R_3P-Au(I)-S=R' have also attracted interest, due to their potential for biological and photophysical applications. [21,22,23,24,25] Thiosemicarbazones and their metal complexes have been the subject of numerous studies because of their chemical and biological properties. The square planar gold(III) complexes with thiosemicarbazones and complexes containing both gold(III) and gold(I) centers are known. In the reports on thiosemicarbazone derivatives of Au(III), the role of stabilizing organometallic ligands and formation of additional Au-C-bond have been discussed.[26,27]

Hard donor ligands, such as nitrogen compounds, favor simple addition reactions to Au(III) centers. With soft donors, reduction of the metal center usually takes place as a consequence of addition/reductive elimination. In this study, we wanted to further clarify the subtle modifications of donor properties and their impact on reaction pathways. In our previous studies we have concentrated on thione ligands with mixed S/N-donor moieties, reduction of the metal center was observed. [28] Now we have brought a N/N heteroatom system into contact with the thione group by investigating the reactions of $AuCl_3$ and $Na[AuCl_4]$ with N,N´-tetramethylthiourea and 2-mercapto-1-methyl-imidazole.

2. Results and Discussion

2.1. Experimental crystal structures

Tetramethylthiourea reacted at room temperature with $AuCl_3$ leading to a formation of an orange solution, which was crystallized at low temperature (-20°C), giving orange crystals of [$AuCl_3$(N,N´-tetramethylthiourea)] (1). The crystallographic details are summarized in Table 1 and the selected geometric parameters are presented in Table 2. The structure of **1** is shown in Fig. 1. This compound has been patented for catalytic applications, but the crystal structure has not been published.[29] Oxidation state III was maintained in the attachment of the ligand, which is rather unusual for thiourea derivatives of gold, as this type of reaction often involves reduction of the gold center. Gold(III) structures with three halide ligands and a sulfur ligand are known but not very common.[15-19,30] The structure of **1** closely resembles these known structures. Gold has almost square planar coordination with S-Au-Cl(1) 176.879(1)°, Cl(3)-Au-S 91.37(6)° and Cl(2)-Au-Cl(1) 89.89(6)°. The Au-S bond length is 2.316(2) Å, which represents typical experimental values for Au-S bond lengths and is considerably smaller than the sum of the van der Waals radii for gold and sulfur (3.46Å). The shortening effect has been contributed to by the presence of additional dπ-dπ back-bonding with σ bond. The S-C(1) bond length is 1.748(7)Å, which is longer than the typical C=S double bond, and resembles C-S single bonds (typical C=S 1.61Å, C-S 1.83Å).[31] The torsion angles Cl-Au-S-C(1) are -173.2(10)°; -36.9(2)° and 145.0(2)° for Cl(1)-Cl(3), respectively. The Au-Cl lengths are in the range of 2.282(2) to 2.306(2)Å, the longest being responsible for Cl(1) *trans* to S. The Au-S-C(1) moiety is bent with a bond angle of 103.7(2)°.

Table 1.

Crystal data and structure refinement for [$AuCl_3$(N,N´-tetramethylthiourea)] (1) and for [$AuCl_3$(2-mercapto-1-methyl-imidazole)] (2) .

	1	2
Empirical formula	$C_5H_{12}AuCl_3N_2S$	$C_4H_6AuCl_3N_2S$
Formula weight	435.54	417.48
Temperature	100(2) K	120(2) K
Crystal system	Monoclinic	Monoclinic
Space group	$P2_1/c$	$P2_1/c$
a (Å)	7.9871(2)	7.7904(7)
b (Å)	10.6839(3)	8.8710(8)
c (Å)	13.5478(3)	13.8471(12)
β°	91.1751(16)	99.088(2)
Volume ($Å^3$)	1155.84(5)	944.94(15)
Z	4	4
Density (calculated)	2.503 Mg/m^3	2.935 Mg/m^3
Absorption coefficient	13.556 mm^{-1}	16.575 mm^{-1}
F(000)	808	760
Crystal size (mm^3)	0.198 x 0.097 x 0.056	0.282 x 0.260 x 0.173
Theta range for data collection	2.428 to 26.494°.	2.648 to 27.520°.
Index ranges	-10<=h<=9, -12<=k<=13, -16<=l<=17	-10<=h<=6, -11<=k<=10, -17<=l<=16
Reflections collected	19313	7397
Independent reflections	2388 [R(int) = 0.0359]	2149 [R(int) = 0.0257]
Completeness to theta = 25.242°	100.0 %	99.4 %
Max. and min. transmission	0.5173 and 0.1744	0.7456 and 0.3071
Data / restraints / parameters	2388 / 0 / 113	2149 / 0 / 101
Goodness-of-fit on F^2	1.126	1.083
Final R indices [I>2sigma(I)]	R1 = 0.0286, wR2 = 0.0665	R1 = 0.0208, wR2 = 0.0534
R indices (all data)	R1 = 0.0328, wR2 = 0.0683	R1 = 0.0233, wR2 = 0.0543
Extinction coefficient	n/a	n/a
Largest diff. peak and hole e.$Å^{-3}$	2.864 and -1.563	1.680 and -1.645

[a] $R1 = \Sigma||F_o| - |F_c||/\Sigma|F_o|$. [b] $wR2 = [\Sigma[w(F_o^2 - F_c^2)^2]/ \Sigma[w(F_o^2)^2]]^{1/2}$.

Table 2.

Selected bond lengths [Å] and angles [°] for [$AuCl_3$(N,N´-tetramethylthiourea)] (1)

Au(1)-Cl(2)	2.282(2)
Au(1)-Cl(3)	2.291(2)
Au(1)-Cl(1)	2.306(2)
Au(1)-S(1)	2.316(2)
S(1)-C(1)	1.748(7)
N(1)-C(1)	1.323(8)
N(2)-C(1)	1.338(8)
Cl(1)-H(2B)	2.7102(0)
Cl(1)-H(3B)	2.8725(1)
Cl(2)-H(4B)	2.8266(1)
Cl(3)-H(4A)	2.8623(1)
Cl(1)-Cl(1)’	3.4333(1)
Cl(1)-Au(1)-S(1)	176.879(1)
Cl(2)-Au(1)-Cl(1)	89.89(6)
Cl(3)-Au(1)-S(1)	91.37(6)
C(1)-S(1)-Au(1)	103.7(2)
C(3)-N(1)-C(2)	113.1(5)
C(4)-N(2)-C(5)	114.6(5)
N(1)-C(1)-N(2)	120.9(6)

Symmetry transformations used to generate equivalent atoms: A: x, 0.5-y, 0.5+z; B: 1-x, -y, 1-z; C: 1-x, -0.5+y, 0.5-z.

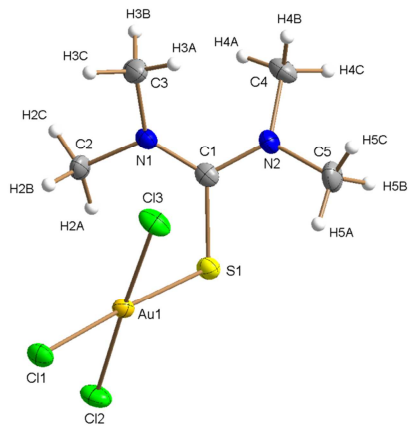

Fig. 1. Structure and numbering scheme of [$AuCl_3$(N,N´-tetramethylthiourea)] (1)

In the solid state of **1** four molecules form units, which are supported by weak hydrogen bonds Cl(1)-H(2B) 2.7102(2)Å, Cl(1)-H(3B) 2.8725(2)Å and Cl(3)-H(4A) 2.8623(1)Å (Fig. 2). Additional Cl(1)···Cl(1) contacts with a distance of Cl(1)-Cl(1) 3.4333(1)Å between the neighboring molecules are found in these units. The distance is diminished by 2% compared to the sum of the van der Waals radii (3.5Å) and the existence of a weak amphoteric halogen bond can be assumed. In this type of interaction the chlorine atoms simultaneously act as electron donors and acceptors.[32] These tetrameric units form an extended chain structure with weak interactions Cl(2)-H(4B) 2.8266(1)Å. It can be suggested that the chloro ligands have the key role in the formation of the supramolecular structure.

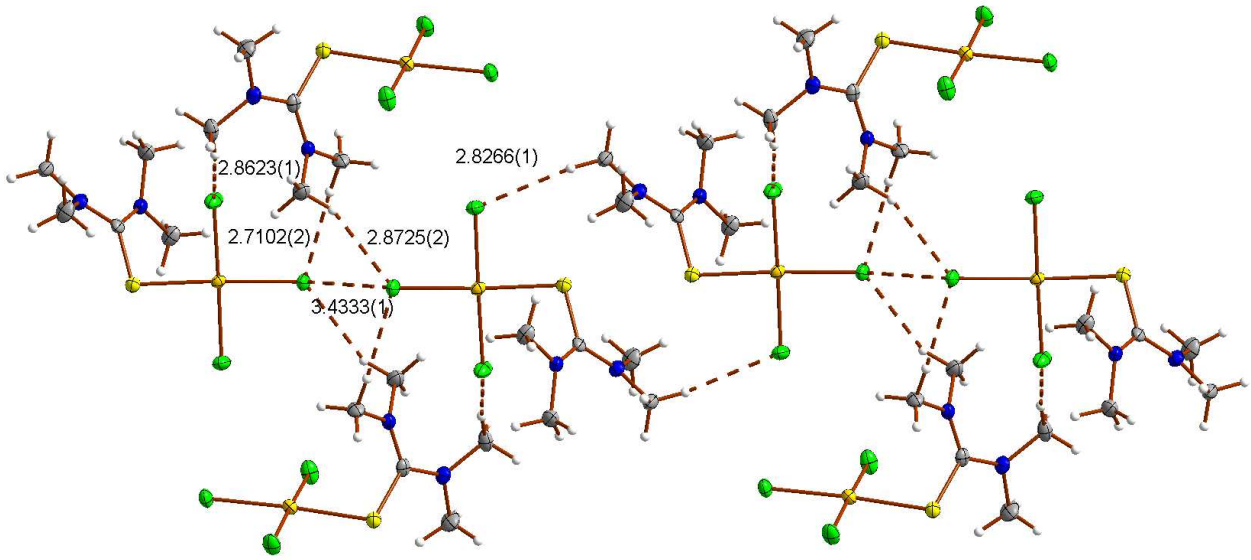

Fig. 2. Chain structure supported by weak hydrogen bonds and amphoteric halogen bond for **1**.

Reaction of 2-mercapto-1-methyl-imidazole with $Na[AuCl_4]\cdot H_2O$ gave orange crystals of [$AuCl_3$(2-mercapto-1-methyl-imidazole)] (2) in good yield. The bond length and bond angle data is given in Table 3. The structure of **2** is shown in Fig. 3. Compound **2** is a monomer with the ligand coordinated by a sulfur atom to central Au(III) with Au-S 2.3179(11)Å and S-C(1) 1.729(4)Å. The distances are close to the corresponding values in **1**, showing similar coordination mode and strength. The coordination sphere of the gold atom is completed with the three chloro ligands Au(1)-Cl(2) 2.2809(11)Å, Au(1)-Cl(3) 2.2810(10)Å and slightly longer Au(1)-Cl(1) 2.3251(11)Å. The S-Au-Cl(1) angle is 174.54(4)° and the Au-S-C(1) bond angle is 105.64(14)°. The Cl(2)-Au(1)-S(1) 84.52(4)° and Cl(3)-Au(1)-S(1) 95.55(4) support the formation of a square planar coordination sphere, similarly to **1**. The torsion angles Cl-Au-S-C(1) are -141.08(3)°; -168.752(3)°

and 13.564(3)° for Cl(1)-Cl(3), respectively.

Table 3.

Selected bond lengths [Å] and angles [°] for [$AuCl_3$(2-mercapto-1-methyl-imidazole)] (2)

Au(1)-Cl(2)	2.2809(11)
Au(1)-Cl(3)	2.2810(10)
Au(1)-S(1)	2.3179(11)
Au(1)-Cl(1)	2.3251(11)
S(1)-C(1)	1.729(4)
N(1)-C(1)	1.345(5)
N(2)-C(1)	1.341(6)
Cl(3)-H(2a)	2.8319(2)
Cl(1)-H(2)	2.4730(2)
Cl(3)-H(2B)	2.7580(2)
Cl(1)-H(3)	2.8936(2)
Cl(2)-Au(1)-Cl(3)	177.69(4)
Cl(2)-Au(1)-S(1)	84.52(4)
Cl(3)-Au(1)-S(1)	95.55(4)
Cl(2)-Au(1)-Cl(1)	90.64(4)
Cl(3)-Au(1)-Cl(1)	89.38(4)
S(1)-Au(1)-Cl(1)	174.54(4)
C(1)-S(1)-Au(1)	105.64(14)

Symmetry transformations used to generate equivalent atoms:
#1 -1+x, 1.5-y, -0.5+z; #2 1-x, -0.5+y, 0.5-z; #3 x, 1.5-y, -0.5+z

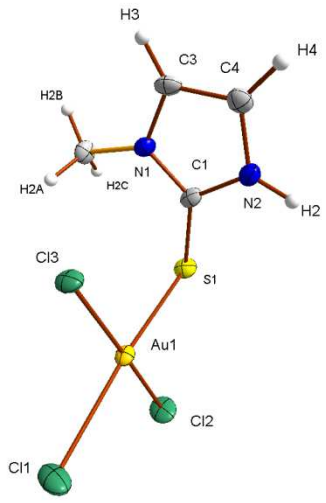

Fig. 3. Structure of [$AuCl_3$(2-mercapto-1-methyl-imidazole)] (2)

In the solid state of **2,** there is a weak intramolecular hydrogen bond Cl(3)-H(2A) 2.8319(2)Å (Fig. 4a). Intermolecular Cl-H hydrogen bonds prevail to give a 3D supramolecular structure. The shortest and thus the strongest interaction is between the chloro ligand and the hydrogen at imidazole nitrogen Cl(1)-H(2) 2.4730(2)Å, whereupon a 1D chain is formed at the ac-plane. The structure is further expanded, when weak interaction between chlorine and a ring hydrogen Cl(1)-H(3) 2.8936(2)Å connect the adjacent zig-zag chains. The final 3D network is gained by weak contact between chlorine and methyl hydrogen Cl(3)-H(2B) 2.7580(2)Å.

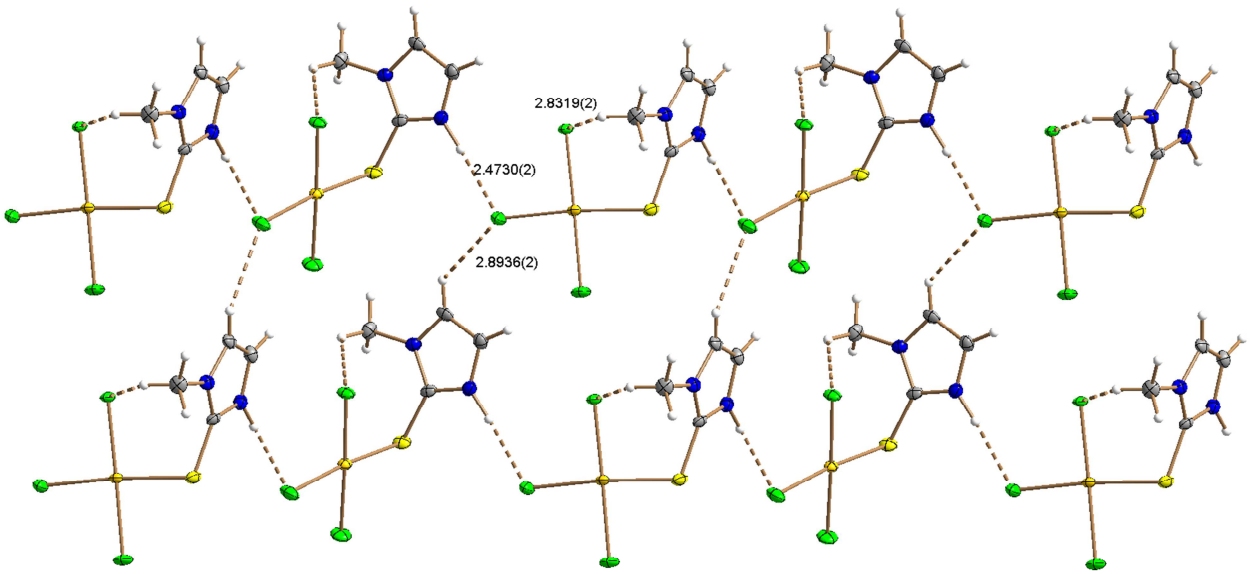

a

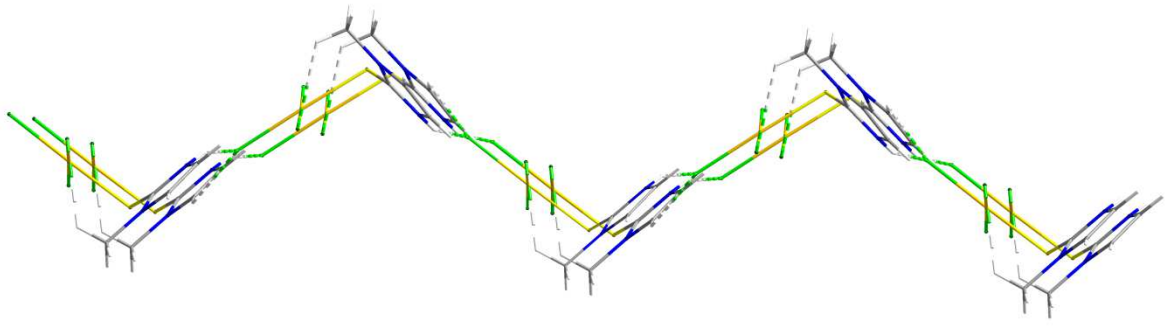

b

Fig 4. 2D structure for **2** at the ac plane (a) and the bc plane (b)

The coordination process of neutral sulfur ligands to the Au(III) center generally depends on the metal to ligand ratio. The relative rates of reduction and substitution define the stoichiometry of the product. To study this behavior, we also carried out reactions with a metal:ligand ratio of 1:2. However, **1** and **2** were obtained from a one hour reaction at room temperature and successive crystallization at low temperature. In a separate test, **1** was stirred with tetramethylthiourea (1:1) in CH_2Cl_2 for 48 h at room temperature, whereby the orange color slowly vanished suggesting reduction of gold. The idea of the formation of a new Au(I) complex e.g. [AuCl(tetramethylthiourea)] (1b) was also supported by the growth of an additive signal at a higher field (3.23 ppm) in the ^{1}H NMR spectrum. The shift is linked to reduction of gold and thus higher electron density at Au(I) compared to Au(III). The growth of the signal was also detected when **1** was stored several months in air, showing partial reduction. However, several attempts to purify and characterize the product in detail failed. In these conditions, the formation of stable solid Au(III) species is favored even though in solution and in precipitated product both Au(I) and Au(III) species are present. In the case of the second reaction, similar behavior was observed; the minor ^{1}H signals of the reduction product, e.g. [AuCl(2-mercapto-1-methyl-imidazole)] (2b), appeared at higher field. In our previous study with a N-methylbenzotiazolidinethione ligand, a similar balance between two oxidation states was observed, but the product with an Au(I) center was crystallized.[28]

2.2. *Computational TD-DFT studies*

In order to verify the oxidation state of gold, and its effect on the solid state structures, we performed computational DFT calculations on the single molecules of **1** and **2**, and also the corresponding hypothetical Au(I) compounds **1b** and **2b**. The optimized structures with possible intramolecular interactions for the molecular compounds are presented in Fig. 5. For comparison, the above-mentioned structures of hypothetical [$AuCl_3$(N-methylbenzotiazolidinethione)] (3a) and structurallycharacterized [AuCl(N-methylbenzotiazolidinethione)] (3b) were included in computational studies.[28]

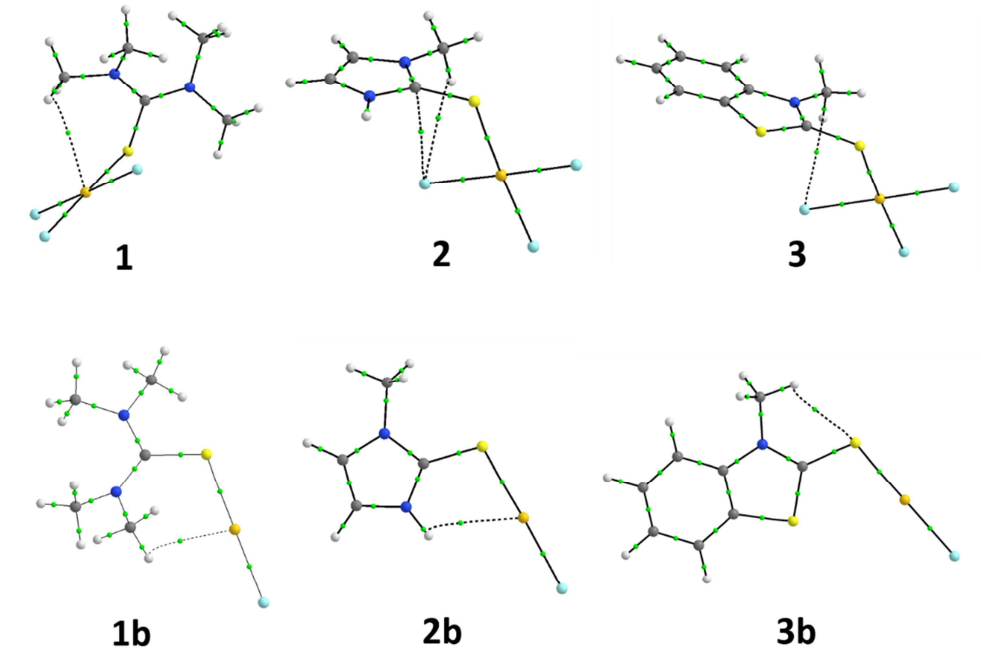

Fig. 5. Optimized structures of Au(III) complexes **1**, **2**, and **3**, and Au(I) complexes **1b**, **2b**, and **3b**. Dashed lines represent non-covalent intramolecular interactions obtained via the QTAIM method, and small green dots the corresponding bond critical points.

The experimental UV-VIS spectra showed charge transfer absorbance at 328 and 241nm for **1**, and the wavelengths of the largest bands for **2** were 353 and 224 nm, as can be seen in Table 4 and in the experimental details. A detailed analysis of the UV-Vis bands was performed by simulating the corresponding spectra in the CH_2Cl_2 solvent with the TD-DFT method. Table 4 lists the most important excitations and their properties. The simulated spectra can be found as supporting information (Figures S1 and S2).

Table 4.

The most important excitations in the UV-Vis spectra of Au(III) complexes **1** and **2**. The properties have been compared with calculated Au(I) complexes [AuLCl], where L=tetramethylthiourea (**1b**) or 2-mercapto-1-methyl-imidazole (**2b**). λ = wavelength (experimental values in parenthesis), f = oscillator strength

Complex	λ (nm)	f	interpretation
1	472	0.0025	HOMO-1=>LUMO(94%)
	342 (328)	0.1078	HOMO-5=>LUMO(40%); HOMO-4=>LUMO(46%)
	232 (241)	0.2796	HOMO=>LUMO+1(95%)
1b	275	0.1048	HOMO=>LUMO(92%)
	250	0.0922	HOMO-2=>LUMO(65%), HOMO-1=>LUMO(24%)
2	487	0.0069	HOMO-1=>LUMO(25%); HOMO=>LUMO(74%)
	361 (353)	0.1972	HOMO-5=>LUMO(51%); HOMO-1=>LUMO(29%)
	225 (224)	0.3652	HOMO-11=>LUMO(76%)
2b	250	0.3497	HOMO=>LUMO(97%)

The calculated excitation energies were similar to the experimental values, thus they support the interpretation of the bands. In particular, the oxidation state of gold in the complexes could be seen in the larger wavelengths of the spectra of **1** and **2** rather than in the corresponding Au(I) complexes **1b** and **2b** (Table 4), even though the lowest energy bands (at 472 nm and 487 nm for **1** and **2**, respectively) were very weak and could only be seen in the experimental spectra as strong tailing of the bands.

Fig. 6. shows the appearance of the MOs in complex **1** that correspond to the excitations in Table 4. The representation of the MOs for compounds **1b**, **2** and **2b** can be seen in Figures S3 and S4.

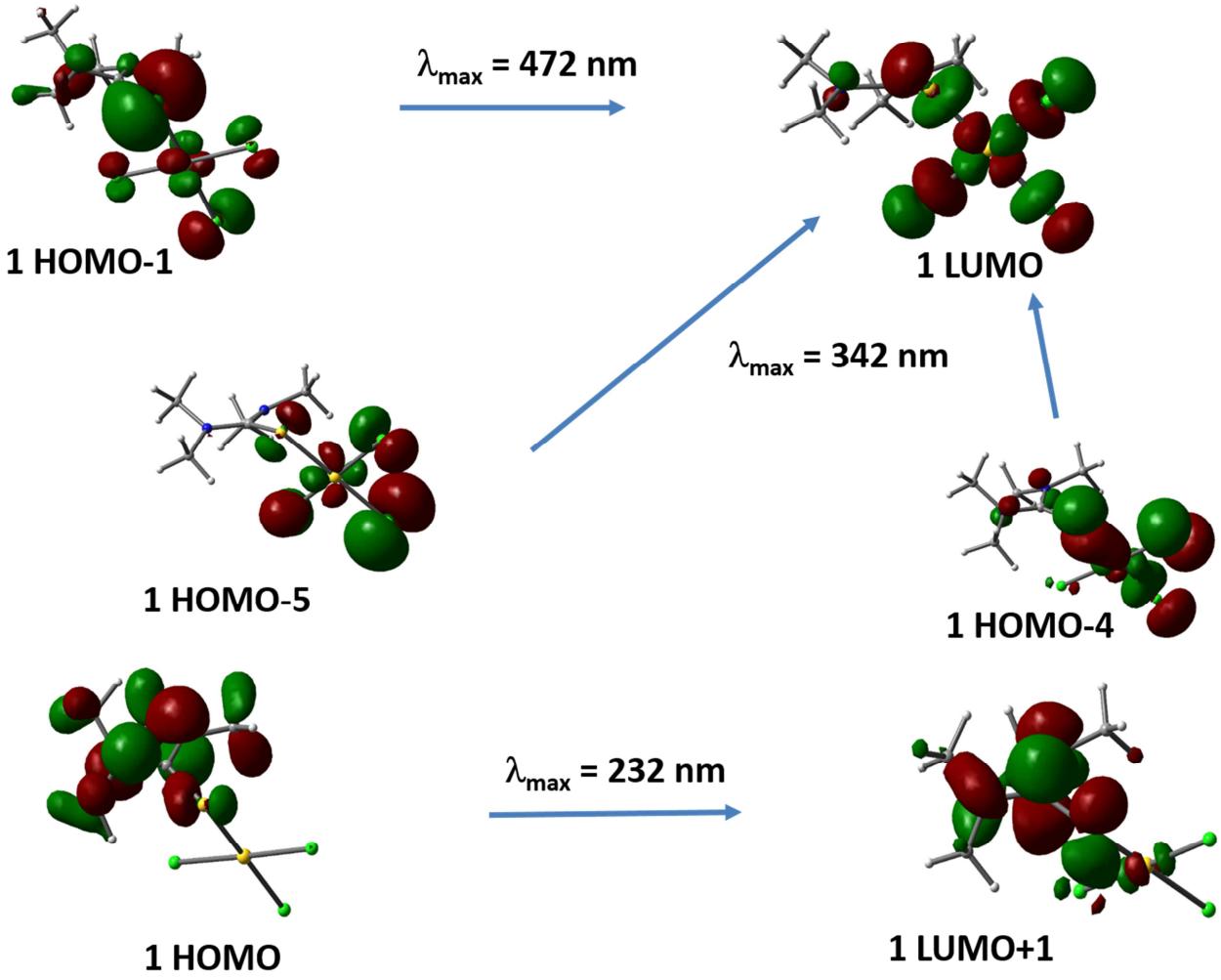

Fig. 6. The appearance of the molecular orbitals, which give rise to the most important excitations in the UV-Vis spectra in **1**. For detailed interpretation of the bands, see Table 4.

The HOMOs are mostly concentrated in the axial direction, with a large contribution to it from both thione sulfur and the chlorine *trans*. The gold d-orbitals take part in forming these higher occupied molecular orbitals. LUMO is represented by the orbitals at the square planar plane of sulfur, gold and the three chlorines, therefore verifying the importance of the donor properties of thione sulfur in the charge transfer process. Furthermore, since the contribution of the Cl(1) *trans* to thione S is slightly larger than that of the other two chlorines, more charge is transferred *via* the axial line. However, the most striking difference in the frontier molecular orbitals between Au(III) and Au(I) complexes can be seen in the constitution of LUMO, which in Au(III) compounds is almost completely concentrated on the S-Au-Cl_3 plane (Fig. 6 and S3-S4), but in the Au(I) complex it is mainly spread over the ligand. The contribution from the metal orbitals stabilizes the LUMO, which is the main reason for smaller energies in the excitations with Au(III) complexes **1** and **2**. On

the other hand, in the Au(I) complexes the possibility for intramolecular hydrogen bonding interactions between Au and H(Me) or H(N) from the N,N ligands stabilizes the HOMO energies, therefore leading to larger energies (and smaller wavelengths) for excitations for **1b** and **2b**.

The experimental IR spectrum of **1** and **2** showed C-N vibrations at 1587 and 1475 cm^{-1} and S-C vibrations at 1497 and 1168 cm^{-1}, respectively. However, the oxidation state of gold could not be deduced from the IR spectra only, since the computational simulation showed only very minor differences in the bands of the Au(III) and Au(I) compounds. The calculated spectra are shown as supporting information in Figures S5 and S6.

Topological charge density analysis

Properties of the electron density around each nuclei can give a lot of information regarding the existence and nature of the intra- and intermolecular interactions in the solid state structures. We analyzed the charge density by using Bader's Quantum Theory of Atoms in Molecules (QTAIM)[40], which has been successfully used to study the nature of these normally weak interactions. For the first stage, we studied the electronic properties of free ligands and how these properties change in the formation of either Au(I) or Au(III) complexes with structurally rather similar N,N ligand 2-mercapto-1-methyl-imidazole (complexes **2b** and **2**) or N,S ligand N-methylbenzotiazolidinethione (**3b** and **3**). The results are listed for selected bond critical points in Table 5. The structures of the optimized complexes with the bond paths and bond critical points are shown in Fig. 5 The numbering of the atoms in Table 5 follows the numbering scheme in Figures 1 and 3.

Table 5.

Selected computational parameters for the optimized Au(I) and Au(III) complexes. d = optimized distance (Å), q= atomic charge according to the AIM analysis, ρ = electron density ($eÅ^{-3}$) at the corresponding bond critical point (BCP), |V|/G = ratio of the potential energy density and the kinetic energy density, E_{int} = interaction energy ($kJmol^{-1}$) at the BCP, δ = delocalization index (bond index) at the BCP. (2-mercapto-1-methyl-imidazole=mmim, N-methylbenzotiazolidinethione=mbtt)

parameter	free ligands		Au(I) complex		Au(III) complex	
	mmim(N,N)	mbtt(N,S)	**2b**(N,N)	**3b**(N,S)	**2**(N,N)	**3**(N,S)
d(C1-S1)	1.669	1.650	1.705	1.689	1.725	1.715
d(S1-Au)	-	-	2.304	2.292	2.365	2.369
q(C1)	0.597	-0.025	0.717	0.045	0.802	0.151
q(S1)	-0.030	0.124	0.139	0.220	0.129	0.187
q(Au)	-	-	0.124	0.159	0.611	0.612
q(Cl1)[a]	-	-	-0.503	-0.497	-0.424	-0.415
ρ(C1-S1)	1.421	1.469	1.398	1.436	1.367	1.389
ρ(S1-Au)	-	-	0.722	0.736	0.660	0.651
|V|/G(C1-S1)	1.98	1.94	2.33	2.27	2.61	2.56
|V|/G(S1-Au)	-	-	1.50	1.49	1.57	1.55
E_{int}(C1-S1)	-658	-702	-563	-600	-488	-510
E_{int}(S1-Au)	-	-	-165	-173	-127	-126
δ(C1-S1)	1.51	1.63	1.30	1.39	1.19	1.27
δ(S1-Au)	-	-	1.00	0.98	0.85	0.82

[a] Cl *trans* to thione S

Initially, the ligands exhibit rather different charge distributions at the C(1)-S(1) bond, originating from the different resonance effect of the aromatic ring systems. When the complexes are formed, both S(1) and C(1) become more positive when electron density is donated to gold ions. The change in the charge was larger for the N,N ligands, again an indication of larger electron donation, which can be understood to facilitate formation of the Au(III) complex. However, the different resonance effect does not solely explain why the N,N ligands are crystallizing in the Au(III) oxidation state

and N,S ligands preferably as Au(I) complexes, since the calculations indicated that the molecular compounds with different oxidation states should be rather similar for both N,N and N,S ligands. The larger electron density at the S(1)-Au bond, the larger interaction energy, and the larger bond delocalization index all indicate stronger interaction and more stability for the Au(I) complexes. In addition, experimental findings indicated that both oxidation states are present in solution, which means that the stability of the complexes would be rather similar.

Another aim was to obtain information on the interactions which determine the crystallization of the Au(III) compounds **1** and **2**. The extended model of the crystal structure of **2** including four molecules at the same layer is shown in Fig. 7a. The results were compared to a previously studied crystal structure of Au(I) compound **3b** with an N-methylbenzotiazolidinethione ligand (Fig. 7b).[28] It should be noted that also larger models, including 7 or 8 molecules for **1** and **2**, respectively, in two adjacent layers, were calculated in order to study the intermolecular interactions between the layers. The larger models are presented as supplementary material (Figures S7 and S8)

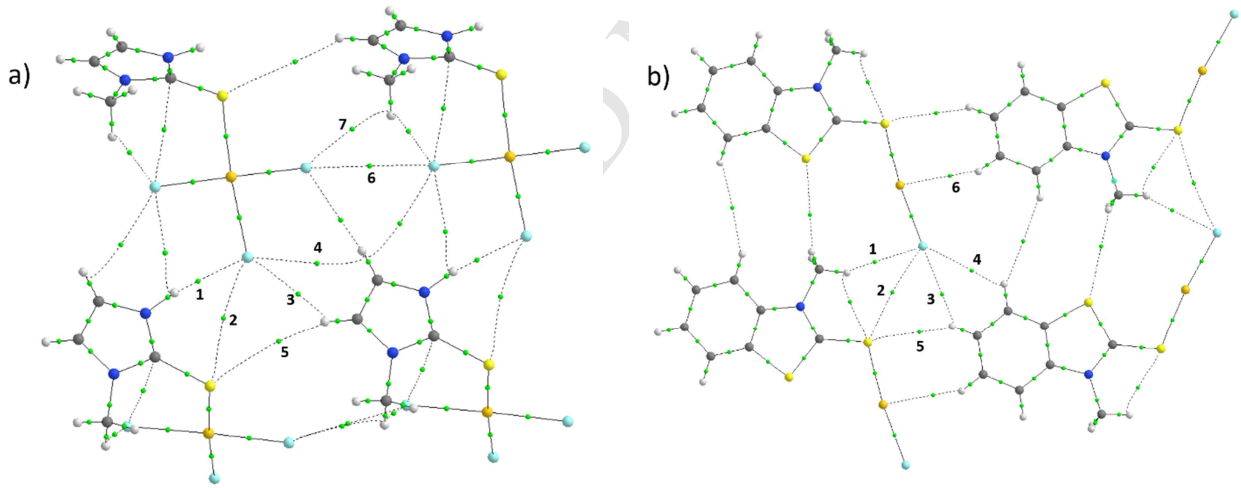

Fig 7. Bond paths and bond critical points (BCPs) in the extended models with four molecules of the crystal structures of compounds a) **2** and b) **3b.** Lines represent the bond paths, and small green dots the BCPs obtained in the QTAIM analysis.

In both structures (and also in the structure of **1**), most of the intermolecular interactions originate from the chlorine *trans* to the thione sulfur (BCPs 1-4 in Fig. 7). This is again an indication of larger charge transfer from the ligand all the way to the Cl(1) atom, which is able to form stronger hydrogen bonding interactions. The H(N) proton of the imidazole ring in **2** forms an especially strong H···Cl interaction (BCP#1, E_{INT} = -18 kJmol^{-1}) compared to H(Me) in **3b** (E_{INT}=-5 kJmol^{-1}), indicating the importance of the (N)H···Cl interaction in stabilizing the crystal structure of **2**. Notably, the optimized molecular structure of a corresponding Au(I) complex [Au(2-mercapto-1-methyl-imidazole)Cl] showed that the H(N) proton is involved in an intramolecular Au···H(N) interaction (Fig. 5), and is not free for further intermolecular interactions. Furthermore, in Au(III) complex **2**, the other two chlorines are able to form amphoteric Cl···Cl contacts (BCP#6), which further stabilize the crystal structure and explain the preferred crystallization of the Au(III) complex over Au(I).

3. Experimental

3.1. Materials and methods

$AuCl_3$ (Alfa Aesar, 64.6% min. metal basis), $Na[AuCl_4]\cdot 2H_2O$ (Alfa Aesar, 99,99%), N,N´-tetramethylthiourea (Aldrich, 98%) and 2-mercapto-1-methyl-imidazole (Aldrich, 98%) were commercially available and used as received. Synthesis of thiourea complex **1** was carried out under a nitrogen atmosphere. The elemental analyses were performed with a varioMICRO V1.7. instrument. ^{1}H and ^{13}C NMR spectra were measured with a Bruker Avance 400 MHz spectrometer and the UV-VIS spectra in CH_2Cl_2 with a Perkin Elmer Lambda 900 UV/VIS/NIR spectrometer.

3.2. Syntheses and analysis

3.2.1. Synthesis of [$AuCl_3$(N,N´-tetramethylthiourea)] (1)

A solution of N,N´-tetramethylthiourea (4.8 mg, 0.041 mmol) in dried methanol (1.0 ml) was added via cannula to $AuCl_3$ (11.7 mg, 0.039 mmol). The mixture was stirred for 40 min affording an orange solution. Diethylether was added, and the solution was left to crystallize at -20°C. Recrystallization from CH_2Cl_2 at -20°C gave orange crystals. Yield 8.0 mg, 51%. ^{1}H NMR ($CDCl_3$): δ 3.35(s, 12H) ppm. ^{13}C NMR 177.9 (S=C), 45.7 (CH_3) ppm. Calc. for $AuCl_3SC_5N_2H_{12}$

C% 13.79; H% 2.78; N% 6.43; S% 7.36. Found C% 13.81; H% 2.67; N% 6.34; S% 6.99. UV-VIS (CH_2Cl_2): strongest signals at 241 nm, 328 nm. IR(KBr): 1497 (ν(C-S)); 1587 (ν(C-N)) cm^{-1}.

3.2.2. Reactivity of [AuCl(N,N´-tetramethylthiourea)] with excess of ligand

A solution of N,N´-tetramethylthiourea (6.6 mg 0.056 mmol, CH_2Cl_2 1.0 ml) was added to the solution of **1** (24.0 mg, 0.055 mmol, CH_2Cl_2 3.0 ml). The mixture was stirred for 48 h until the orange colour disappeared. For **1b**: ^{1}H NMR ($CDCl_3$): δ 3.23 (s) ppm.

3.2.3.Synthesis of [$AuCl_3$(2-mercapto-1-methyl-imidazole)] (2)

$Na[AuCl_4]\cdot 2H_2O$ (60.8 mg, 0.15 mmol) was dissolved in MeOH (2.0 ml) and added to a solution of 2-mercapto-1-methyl-imidazole (17.5 mg, 0.15 mmol) in MeOH (1.0 ml). Crystallization at -20°C gave orange crystals. Yield 38.0 mg, 60%. ^{1}H NMR (Me_2SO-d_6): δ 9.09 (N-H, s, 1H); 7.71 (Ar, s, 1H); 7.68(Ar, s, 1H); 3.88 (CH_3, s, 3H) ppm. ^{13}C NMR 168.0 (S=C), 123.0 (C ring); 119.6. (C ring); 35.3 (CH_3) ppm. Calc. for $AuCl_3SC_4N_2H_6$ C% 11.51; H% 1.45; N% 6.71; S% 7.68. Found C% 11.79; H% 1.63; N% 6.70; S% 7.30. UV-VIS (CH_2Cl_2): strongest signals at 224 nm, 353 nm. IR(KBr): 1168 (ν(C-S)); 1475 (ν(C-N)) cm^{-1}.

For **2b** ^{1}H NMR (Me_2SO-d_6δ 13.60(NH); 7.50 (Ar, 1H); 7.33(Ar, s, 1H); 3.70 (CH_3, s, 3H) ppm.

3.3. X-ray Structure Determinations

The crystals of **1** and **2** were immersed in cryo-oil, mounted in a Nylon loop, and measured at a temperature of 100 and 120K, respectively. The X-ray diffraction data were collected on a Nonius KappaCCD (1) or NoniusKappa Apex II (2) diffractometer, using Mo Kα radiation (λ = 0.710 73 Å). The *Denzo-Scalepack*[33], program package was used for cell refinements and data reductions. The structures were solved by direct methods using the *SHELXS-97*[34] program with the *WinGX*[35]graphical user interface. A semi-empirical absorption correction (*SADABS*)[36] was applied to all data. Structural refinements were carried out with the use of *SHELXL-97*.[34] For both **1** and **2,** hydrogen atoms were positioned geometrically and constrained to ride on their parent atoms, with C-H = 0.95-0.98 Å and U_{iso} = 1.2-1.5 U_{eq}(parent atom). The crystallographic details for **1** and **2** are summarized in Table 1.

3.4. Computational Details

All models were calculated with the Gaussian 09 program package[37] at the DFT level of theory. The hybrid density functional PBE0[38] was utilized together with the basis set, consisting of the def2-TZVPPD[39] effective core potential basis set with a triple-zeta-valence basis set with two sets of polarization and diffuse basis functions for Au atoms, the standard all-electron basis sets 6-311+G(d) for N, S and Cl atoms, and 6-31G(d,p) for C and H atoms. In order to study the electronic and interaction properties of the complexes, we performed topological charge density analysis with the QTAIM (Quantum Theory of Atoms in Molecules) method.[40] This analysis was done with the AIMAll program[41] via the use of wave functions obtained from the DFT calculations. The selected properties were: ρ = local electron density at the BCP; $|V|/G$ = ratio of potential energy density (V) and kinetic energy density (G); E_{INT} = interaction energy between two interacting atoms = 1/2 x V(BCP) as stated by Espinosa et. al.[42] δ(A, B) = delocalization index between two (bonding) atoms; and q(A) = total atomic charge of atom A according to AIM analysis.

Full optimizations were performed on the free ligands and separate complex molecules before the AIM analysis. The more extended models of the solid state structures were directly cut from the corresponding experimental crystal structures and analyzed without geometry optimization. Frequency analysis without scaling was performed in order to simulate the IR spectra of the optimized complex molecules, and also to ensure that the optimized structures were minima. Absorption characteristics were studied with the TD-DFT method at the same level of theory as the optimizations. Solvent effects of the CH_2Cl_2 solvent were calculated via the conductor-like polarized continuum model (CPCM).[43]

4. Conclusions

Oxidation state III of gold was preferred in solid state derivatives of N,N´-substituted thiones.
The main reason for the persistence of oxidation state III in a crystalline state was found to be weak intra- and intermolecular hydrogen bond and halogen bond interactions. The effect of the oxidation state on the electronic properties of the compounds was investigated via spectroscopic methods and computational DFT calculations.

5. Acknowledgements

The computational work was facilitated and made available by the Finnish Grid Infrastructure (FGI) resources. Support from COST action CM1302: European Network on Smart Inorganic Polymers (SIPs) is also gratefully acknowledged.

Supplementary material

The crystallographic data for compounds $AuCl_3$(N,N´-tetramethylthiourea) (1) and AuCl3(2-mercapto-1-methyl-imidazole) (2) have been deposited with the Cambridge Crystallographic Data Centre as supplementary publication no. CCDC 796465 and CCDC 1499191. Copies of this information may be obtained free of charge via www.ccdc.cam.ac.uk/data_request/cif. The supplementary material also includes figures of simulated IR and UV-Vis spectra, and bond paths and bond critical points of extended models of **1** and **2**. Supplementary data associated with this article can be found in the online version, at doi: XXX.

References

[1] Z.E. Nazari, M. Banoee, A.A. Sepahi, F. Rafii, A.R. Shahverdi, Gold Bull. 45 (2012) 53-59.
[2] A. Casini, M.C. Diawara, R. Scopelliti, S.M. Zakeeruddin, M. Grätzel, P.J. Dyson, Dalton Trans 39 (2010) 2239-2245.
[3] J.J Yan, R.W.-Y. Sun, P. Wu, M.C.M. Lin, A.S.-C. Chan, C.-M. Che, Dalton Trans 39 (2010) 7700-7705.
[4] B.A. Al-Maythalony, M. Monim-ul-Mehbood, M. Altaf, M.I.M. Wazeer, A.A. Isab, S. Altuwaijri, A. Ahmed, V. Dhuna, G. Bhatia, K. Dhuna, S.S. Kamboj, Spectrochimica Acta Part A: Molecular and Biomolecular Spectroscopy 115 (2013) 641-647.
[5] M. Monim-ul-Mehbood, M. Altaf, M. Fettouhi, A.A. Isab, M.I.M. Wazeer, M.N. Shaikh, S. Altuwaijri, Polyhedron 61 (2013) 225-234.
[6] A. Ericson, L.I. Elding, S.K.C. Elmroth, J. Chem. Soc. Dalton Trans. (1997) 1159-1164.
[7] S.K.C.Elmroth, L.I. Elding, Inorg.Chem. 35 (1996) 2337-2342.
[8] S. Elmroth, L.H. Skibsted, L.I. Elding, Inorg.Chem. 28 (1989) 2703-2710.
[9] (a) S. Friedrichs, P.G.Jones, Acta Crystallogr., Sect.C:Cryst.Struct.Commun. C55 (1999) 1625-1627; (b) M.S. Hussain, A.A. Isab, Transition Met.Chem. 9 (1984) 398-401; (c) M.S. Hussain, A.A. Isab, J.Coord.Chem. 14 **(**1985) 17-26; (d) M.S. Hussain, A.A. Isab, Transition Met.Chem. 10 (1985) 178-181; (e) S. Friedrichs, P.G. Jones, *Z.* Naturforsch.,B:Chem.Sci. 59 (2004) 49-57; (f) P.G. Jones, J.J. Guy, G.M. Sheldrick, Acta Crystallogr.,Sect.B:Struct.Crystallogr.Cryst.Chem. 32 (1976) 3321-3322; (g) S. Friedrichs, P.G. Jones, Z.Naturforsch.,B:Chem.Sci. 59 (2004) 1429-1437. h. M. Fettouhi, A.A. Isab, M.I.M. Wazeer, Z.Kristallogr.-New Cryst.Struct. 219 (2004) 391-392; (i) M.B. Cingi, F. Bigoli, M. Lanfranchi, E. Leporati, M.A. Pellinghelli, C. Foglia, Inorg. Chim. Acta 235 (1995) 37-43.
[10] (a) W. Bensch, M. Schuster, Z.Anorg.Allg.Chem. 611 (1992) 99-102; (b) F.B. Stocker, D. Britton, Acta Crystallogr.,Sect.C:Cryst.Struct.Commun. c56 (2000) 798-800; (c) R. Richter, U. Schroder, M. Kampf, J. Hartung, L. Beyer, Z.Anorg.Allg.Chem. 623 (1997) 1021-1026; (d) R.J.

Staples, J.P. Jr., Fackler, J. Costamagna, ActaCrystallogr.,Sect.C:Cryst.Struct.Commun. 53 (1997) 1555-1558.
[11] L.C. Porter, J.P. Jr. Fackler, J. Costamagna, R. Schmidt, Acta Cryst. C48 (1992) 1751-1754.
[12] O.E. Piro, E.E. Castellano, R.C.V. Piatti, A.E. Bolzán, A.J. Arvia, Acta. Cryst. Sect. C, Cryst. Struct. Commun. 58 (2002) m252-m255.
[13] C.-C. Lin, S.-X. Liu, R.-S.Yong, H. Jiegou Chin. J. Struct. Chem. 9 (1990) 42.
[14] A.C. Fabretti, A. Giusti, W. Malavasi, J. Chem. Soc. Dalton Trans. (1990) 3091.
[15] P.G. Jones, E. Bembenek, Z.Kristallogr. 208 (1993) 126.
[16] N.W.Alcock, K.P.Ang, K.F.Mok, S.F.Tan; Acta Crystallogr.,Sect.B:Struct.Crystallogr. Cryst.Chem. 34 (1978) 3364-3366.
[17] P.G.Jones, J.Lautner; Z.Kristallogr.208 (1993) 130.
[18] K.Takahashi; Bull.Chem.Soc.Jpn. 64 (1991) 2572.
[19] K.Takahashi, H.Tanino; Chem.Lett. (1988) 641-644.
[20] B. D. Glisic, S. Rajkovc, Z.D. Stanic, M.I. Djuran; Gold Bull. 44 (2011) 91-98.
[21] A.A. Isab, M. Fettouhi, S. Ahmad, L. Ouahab, Polyhedron 22 (2003) 1349-1354. DOI 10.1016/S0277-5387(03)00129-3.
[22] W. Henderson, B.K. Nicholson, E.R.T. Tiekink, Inorg. Chim. Acta 359 (2006) 204-214.
[23] E. Vergara, S. Miranda, F. Mohr, E. Cerrada, E.R.T. Tiekink, P. Romero, A. Mendía, M. Laguna, Eur. J. Inorg. Chem. (2007) 2926-2933.
[24] W. Eikens, P.G. Jones, J. Lautner, C. Thone, Z.Naturforsch.,B:Chem.Sci. 49 (1994) 21-26.
[25] P.D. Cookson, E.R.T. Tiekink, J.Chem.Cryst. 24 (1994) 805-810.
[26] I. Garcia Santos, A. Hagenbach, U. Abram, Dalton Trans. (2004) 677-682.
[27] A. Castineiras, S. Dehnen, A. Fuchs, I. García-Santos, P. Sevillano, Dalton Trans. (2009) 2731-2739.
[28] (a) L. Koskinen, S. Jääskeläinen, P. Hirva, M. Haukka, Cryst Growth and Des. 15 (2015) 1160-1167; (b) L. Koskinen, S. Jääskeläinen, E. Kalenius, P. Hirva, M. Haukka, Cryst Growth and Des. 14 (2014) 1989-1997.
[29] J. Sundermeyer, C. Jost 2001 DE 10041510 A1 20010412.
[30] (a) K.Takahashi, K.Kato, Bull.Chem.Soc.Jpn. 61 (1988) 991; (b) G.A.Nifontova, O.N.Krasochka, I.P.Lavrent'ev, D.D.Makitova, L.O.Atovmyan, M.L.Khidekel, Izv.Akad.Nauk SSSR,Ser.Khim.(Russ.Chem.Bull.) (1988) 450; (c) H.G.Raubenheimer, R. Otte, L.Linford, W.E.van Zyl, A.Lombard, G.J.Kruger, Polyhedron 11 (1992) 893-900; (d) P.G.Jones, J.Lautner, Z.Kristallogr. 208 (1993) 130.
[31] B.V. Trzhtsinskaya, N.D. Abramova, Sulfur reports 10 (1991) 389.
[32] Y.V. Nelyubina, M.Y. Antipin, D.S. Dunin,V.Y.K. Kotov, K.A. Lyssenko, Chem. Commun. 46 (2010) 5325- 5327.
[33] Z. Otwinowski, W. Minor, in Methods in Enzymology, Volume 276, Macromolecular Crystallography, Part A. (Eds. C. W. Carter, J. Sweet) 1997**,** p. 307 (Academic Press: New York, USA).
[34] G. M. Sheldrick, Acta Cryst. A64 (2008) 112-22.
[35] J. Farrugia, J. Appl. Cryst. 32 (1999) 837-838.
[36] G. M. Sheldrick, SADABS - Bruker AXS scaling and absorption correction -, Bruker AXS, Inc., Madison, Wisconsin, USA, 2008
[37] M.J. Frisch, G.W. Trucks, H.B. Schlegel, G.E. Scuseria, M.A. Robb, J.R. Cheeseman, J. G. Scalmani, V. Barone, B. Mennucci, G.A. Petersson, H. Nakatsuji, M. Caricato, X. Li, H.P. Hratchian, A.F. Izmaylov, J. Bloino, G. Zheng, J.L. Sonnenberg, M. Hada, M. Ehara, K. Toyota, R. Fukuda, J. Hasegawa, M. Ishida, T. Nakajima, Y. Honda, O. Kitao, H. Nakai, T. Vreven, J.A. Montgomery, Jr. J.E. Peralta, F. Ogliaro, M. Bearpark, J.J. Heyd, E. Brothers, K.N. Kudin, V.N. Staroverov, R. Kobayashi, J. Normand, K. Raghavachari, A. Rendell, J.C.Burant, S.S. Iyengar, J.

Tomasi, M. Cossi, N. Rega, J.M. Millam, M. Klene, J.E. Knox, J. B. Cross, V. Bakken, C. Adamo, J. Jaramillo, R. Gomperts, R.E. Stratmann, O. Yazyev, A.J. Austin, R. Cammi, C. Pomelli, J.W. Ochterski, R.L. Martin, K. Morokuma, V.G. Zakrzewski, G.A. Voth, P. Salvador, J.J. Dannenberg, S. Dapprich, A.D. Daniels, Ö. Farkas, J.B. Foresman, J.V. Ortiz, J. Cioslowski, D.J. Fox, In Gaussian 09, Revision C.01; Gaussian, Inc: Wallingford CT (2009).

[38] J. P. Perdew, K. Burke, M. Ernzerhof, Phys. Rev. Lett. 78 (1997) 1396-1396.

[39] D. Rappoport, F.J. Furche, Chem. Phys. 133 (2010) 134105/1-11.

[40] R.F.W. Bader, Atoms in Molecules: A Quantum Theory; Oxford University Press: Oxford (1990).

[41] T.A. Keith, AIMAll (Version 12.06.03), TK Gristmill Software; aim. tkgristmill. com: Overland Park, KS, USA (2003).

[42] E. Espinosa, I. Alkorta, J. Elguero, E. Molins, J. Chem. Phys. 117 (2002) 5529-5542.

[43] M. Cossi, N. Rega, G. Scalmani, V. Barone, J. Comp. Chem. 24 (2003) 669-681.

Persistence of oxidation state III of gold in thione coordination.

Sirpa Jääskeläinen[a,*], Laura Koskinen[a], Matti Kultamaa[a], Matti Haukka[b] and Pipsa Hirva[a]

[a] Department of Chemistry, University of Eastern Finland, Joensuu Campus, P.O. Box 111, FI-80101 Joensuu, Finland

[b] Department of Chemistry, University of Jyväskylä, P.O. Box 35, FI-40014 Jyväskylä, Finland

[*]Corresponding author. Tel. +358 505689428. E-mail address: sirpa.jaaskelainen@uef.fi

Highlights

- Thione derivatives of gold were synthesized and characterized
- Oxidation state III was atypically maintained
- Computational TD-DFT studies were used to explain spectroscopic data
- DFT and QTAIM methods were employed to clarify the oxidation state of the metal and the weak interactions in solid state